Solidification Crack Susceptibility in Laser Beam Weld Metal of 0.2C-Low Alloy Steels†

–Effects of Bead Configuration and S and P Contents–

Fukuhisa MATSUDA*, Hiroji NAKAGAWA**, Tomoyuki UEYAMA***

Abstract

Solidification crack susceptibility in partially-melted bead-on-plate laser beam weld metal of 6mm thick 0.2C-1.8Ni-0.55Cr-0.25Mo low alloy steel has been investigated with change of S and P content using a max. 5KW laser beam welder.

Effects of weld bead configuration and amount of S and P on crack length in crosssectional bead have been mainly investigated. Estimation of crack length in weld metal was tried by means of regression analysis of data, using bead configuration and S and P.

Moreover effect of restraint of weld bead during welding on crack susceptibility was investigated.

KEY WORDS: (Solidification Crack) (Laser Beam Welding) (Impurity) (Low Alloy Steel)

1. Introduction

Laser beam welding (LBW) is recently being prevailed for higher carbon low alloy steels, which were unexpectable steels to welding before, by adoption of beneficial features of high energy beam, less distortion and no hydrogen during welding[1, 2, 3]. As a vacuum atmosphere is not required to weld in LBW in comparison with EBW, LBW is much promptly applied to welding of special steels although many features are almost the same as in EBW.

However recently some difficulties were reported, when higher carbon low alloy steels in commercial use were welded with LBW in partially-melted condition. One of the most serious difficulties is solidification crack in weld metal which is caused by amount of impurities as S and P in general. Usually these steels used in machinary parts are not made for the fabrication by welding, then impurities as S and P in these steels are not controlled so strictly.

Therefore the authors have investigated the effects of weld bead configuration in crosssection and contents of S and P on solidification crack susceptibility in partial penetration weld bead in LBW, using a machinary steel of 6mm thick 0.2%C-1.8Ni-0.55Cr-0.25Mo (JIS SNCM 420) whose S and P contents are widely varied. The solidification crack susceptibilities of weld beads whose welding variables were changed were evaluated by crack length in crosssection, and then the equation which can estimate the total crack length in bead was introduced by statistical regression analysis. Moreover the crack susceptibilities between restraint and unrestraint weld beads were compared.

2. Experimental Procedure

2.1 Steels used

Steel used in this investigation is 6mm thick 0.2C-1.8Ni-0.55Cr-0.25Mo (JIS SNCM 420) which is widely used for fabrication of machine parts in Japan. Chemical compositions of the steel in which S and P are individually varied from 0.003 to 0.033% within a limit of JIS specification are shown in **Table 1**.

2.2 Welding variables used

Welding variables have been selected in a range of partial penetration weld bead for 6mm thick plate. A 5KW multimode type CO_2 laser welder is used for all LBW whose welding conditions are shown in **Table 2 (a)** and **(b)**. Table 2 (a) is applied for welding of restraint condition and (b) for without restraint condition. Most of

† Received on Nov. 4, 1987

* Professor
** Research Instructor
*** Daihen Corp., formerly graduate student

Transactions of JWRI is published by Welding Research Institute of Osaka University, Ibaraki, Osaka 567, Japan

Table 1 Chemical composition of materials used.

Chemical composition (wt%)										
C	Si	Mn	P	S	Ni	Cr	Mo	Al	N	O
0.19 ~ 0.20	0.27 ~ 0.30	0.54 ~ 0.58	**0.003 ~ 0.033**	0.005 ~ 0.027	1.76 ~ 1.87	0.53 ~ 0.56	0.23 ~ 0.25	0.010 ~ 0.015	0.0042 ~ 0.0057	0.0011 ~ 0.0016

Table 2 Welding conditions of LBW (a) restraint (b) restraint-free

(a)

Focal length D_F (mm) (Q_b=0.98)	Laser power W_b (kW)	Welding speed v_b (mm/s (mm/min))	Assist gas He (cm^3/s (l/min))
127, 190, 254	2	16.7 (1000)	500 (30)
		25.0 (1500)	830 (50)
		37.5 (2250)	500 (30)
	3	16.7 (1000)	500 (30)
		25.0 (1500)	830 (50)
		37.5 (2250)	830 (50)
		68.8 (4125)	500 (30)
	5	35.3 (2115)	830 (50)
		45.8 (2750)	830 (50)
		68.8 (4125)	830 (50)

(b)

Focal length D_F (mm) (Q_b=0.98)	Laser power W_b (kW)	Welding speed v_b (mm/s (mm/min))	Assist gas He (cm^3/s (l/min))
127	3	16.7 (1000)	500 (30)
	5	35.3 (2115)	

this investigation are welded under the restraint fixture, however, in order to compare the solidification crack susceptibility with the restraint free condition, some are welded under the restraint free.

Specimen size for one weld bead is 130 (in length) × 100mm (in width) × 6mmt.

Restraint fixture used for welding of restraint condition is shown in **Fig. 1**.

Partially penetration bead was laid on the center of the specimen longitudinally as shown in Fig. 1.

Helium assisting gas of 500 and 800cm^3/sec was flown to the location of laser injection in order to remove plasma generated during welding.

2.3 Measurement of cracking length in weld bead

Middle part of each weld bead was cut as shown in **Fig. 2**, and the total crack length C_T was measured as an aver-

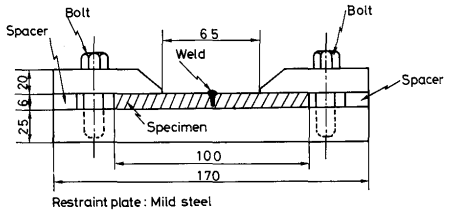

Fig. 1 Shape and size of restraint fixture made of mild steel used in LBW.

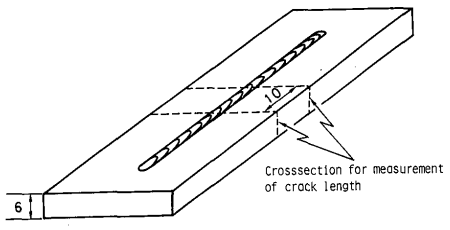

Fig. 2 Sampling location of specimens for analysis of total crack length, and micro and macro structure.

age of 2 sections by means of an optical microscope × 50 magnification after polished up to 0.3μm alumina powder and etched with saturated picral.

Moreover, in order to analyse crack susceptibility in weld bead, sum of crack lengths in both parts of "nail head" and "well" in crosssection of bead was separately measured as C_{TN} and C_{TW} besides C_T (= C_{TN} + C_{TW}) which are shown in **Fig. 3**. The reason why C_{TN} and C_{TW} were measured is that cracking in "nail head" part would be little delayed in time after cracking in "well" part judging from configuration of crosssectional bead.

3. Experimental Results

3.1 Configuration of weld bead

Figure 4 shows typical bead configurations which were seen in this investigation. They are divided into four types, (a) for "winecup", (b) for "well", (c) for "pear" and (d) for "semi-sphere" shaped. Most of weld beads,

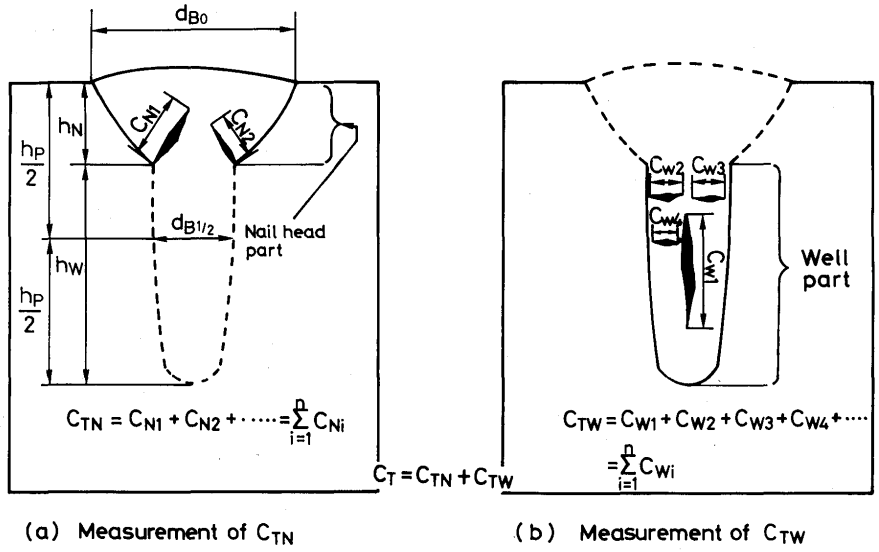

Fig. 3 Definition of total crack length in nailhead part, C_{TN}, and in well part, C_{TW}, in LBW.

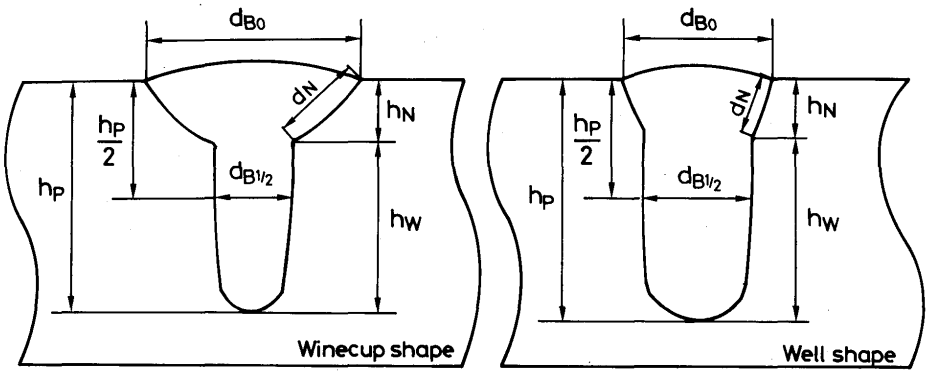

Fig. 5 Definition of penetration parameters to describe penetration shape.

however, show (a) and (b) types in this investigation. Cracks mainly occur obliquely from lower part of the nail head for (a), horizontally in the middle and lower part of bead penetration for (b) and vertically in the center of bead for (c), and no crack occurs for (d). Cracks in (b) are generally much more than those in (a). All these cracks show the feature pattern of solidification cracking in fractographic investigation[4].

Now the authors have defined the symbols in crosssectional bead as in **Fig. 5**.

The relation between two parameters d_{B0}/h_N and $h_w/d_{B1/2}$ and bead configuration is shown in **Fig. 6** at the same penetration depth. Higher d_{B0}/h_N and lower $h_w/d_{B1/2}$ shows winecup type, and the reverse shows well type bead.

All weld beads for a kind of steel are shown in the above two parameters as shown in **Fig. 7** with number of $d_{B0}/d_{B1/2}$. According to Fig. 7, a parameter $d_{B0}/d_{B1/2}$ also shows well the bead configuration, that is, increasing $d_{B0}/d_{B1/2}$ shows winecup and decreasing well type bead. Now

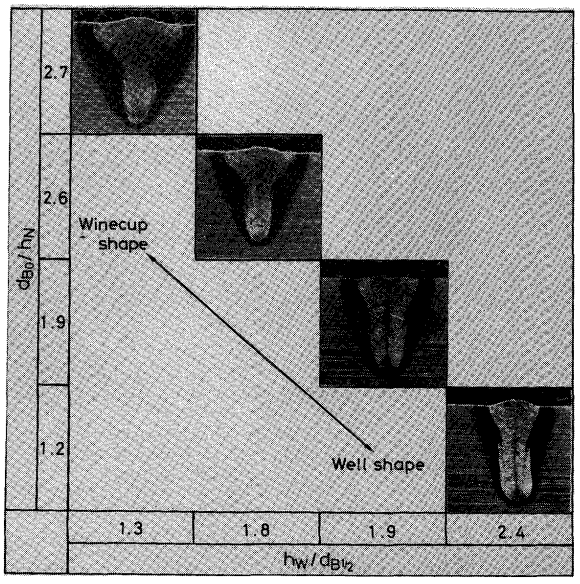

Fig. 6 Relation between penetration parameters and penetration shape.

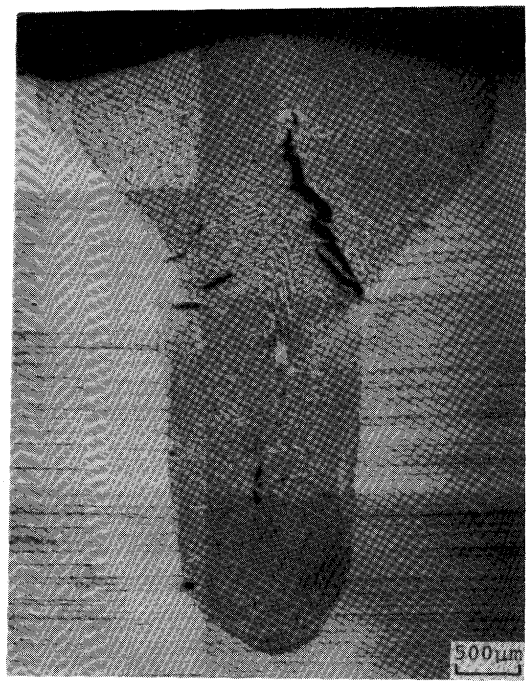

(a) Winecup shape
W_b:5kW, v_b:16.7mm/s
D_F:127mm, a_b:0.98
S:0.027%, P:0.019%

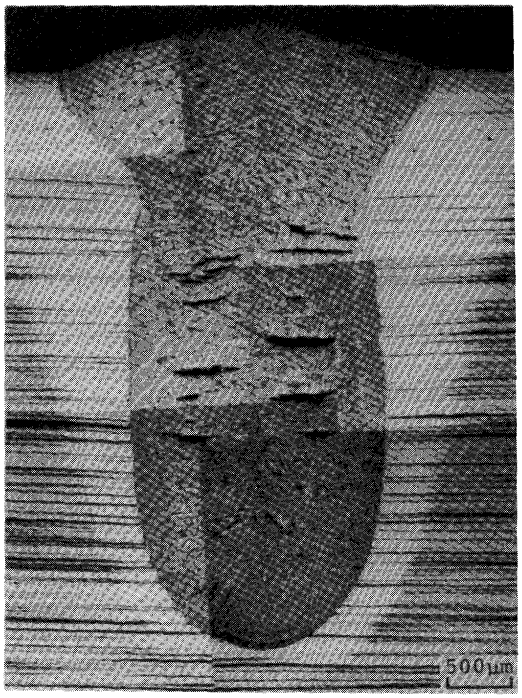

(b) Well shape
W_b:5kW, v_b:35.3mm/s
D_F:190mm, a_b:0.98
S:0.027%, P:0.003%

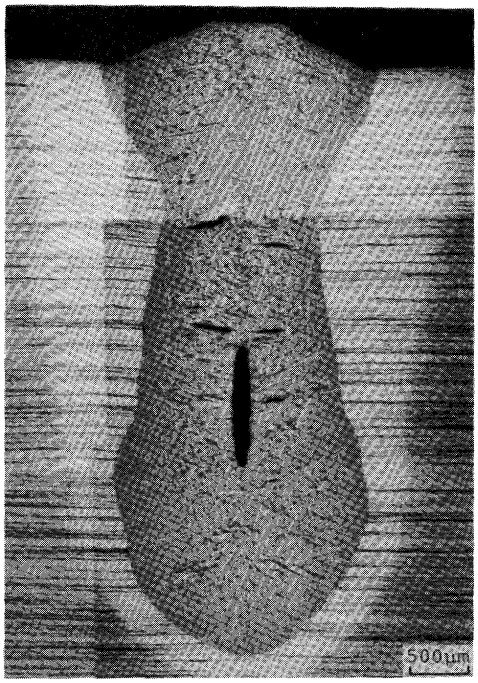

(c) Pear shape
W_b:5kW, v_b:45.8mm/s
D_F:127mm, a_b:0.98
S:0.011%, P:0.011%

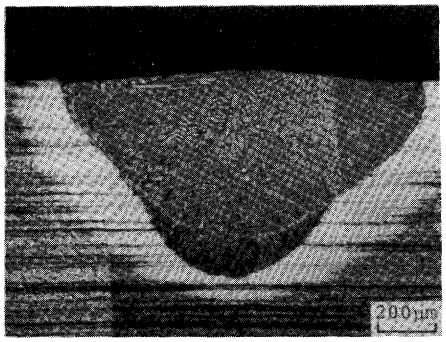

(d) Semi-spherical shape
W_b:3kW, v_b:68.8mm/s
D_F:254mm, a_b:0.98
S:0.024%, P:0.033%

Fig. 4 Typical examples of weld bead configuration and crack in each penetration type.

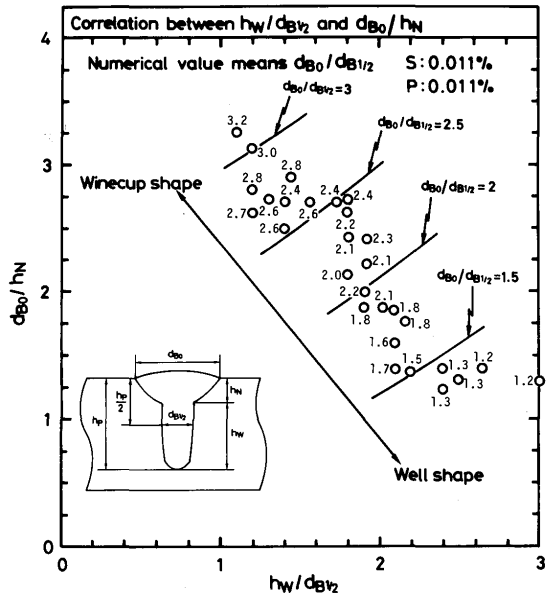

Fig. 7 Relation among $h_W/d_{B1/2}$, d_{Bo}/h_N and $d_{Bo}/d_{B1/2}$.

the authors have defined winecup type for more than 2 of $d_{Bo}/d_{B1/2}$ parameter and well type for less than and including 2.

Figure 8 shows the relations between welding variables and bead configurations by $d_{Bo}/d_{B1/2}$. An increase in power and or welding speed shows well type bead with decreasing of $d_{Bo}/d_{B1/2}$. Effect of focal length is not so obvious. Pear type bead tends to occur in higher power, higher welding speed and shorter focal length, semi-spherical type bead occurs in lower power, higher speed and longer focal length. As there is no cracks due to very shallow penetration (<0.7mm) in semi-spherical type bead, the authors have omitted hereafter in consideration of crack susceptibility.

Laser power W_b (kW)	Focal length D_F (mm) (a_b=0.98)	Welding speed, v_b (mm/s (mm/min)) 16.7 (1000)	25 (1500)	35.3-37.5 (2115-2250)	45.8 (2750)	68.8 (4125)
2	254	3.2	2.8	2.4	$d_{Bo}/d_{B1/2}$ decreasing	
	190	3.0	2.6	2.3		
	127	2.8	2.4	2.3		
3	254	2.6	2.4	2.3		1.4
	190	2.6	2.4	2.1		1.8
	127	2.3	2.2	1.8		1.5
5	254	Numerical value means $d_{Bo}/d_{B1/2}$		1.8	1.7	2.0
	190			1.7	1.6	1.3
	127			1.3	1.2	1.2

Winecup shape $d_{Bo}/d_{B1/2} > 2$ — Well shape $d_{Bo}/d_{B1/2} \leqq 2$

Pear shape — Semi-spherical shape

Fig. 8 Relation between welding condition and $d_{Bo}/d_{B1/2}$.

3.2 Total crack length, C_T, vs. welding variables and bead configurations

3.2.1 C_T vs. welding variables

Figure 9 (a), (b) and **(c)** show the effect of individual welding speed, laser power and focal length on C_T in which parameter $d_{Bo}/d_{B1/2}$ is simultaneously shown. An increase in welding speed and laser power increases C_T, but that of focal length does not obvious. The $d_{Bo}/d_{B1/2}$ behaves a good correlation to C_T in reverse fashion. Moreover **Fig. 10 (a)** and **(b)** show the same relations for weld beads whose penetration depth is almost a constant of 3.0mm. In these results an increase in welding speed and laser power also increases C_T and decreases $d_{Bo}/d_{B1/2}$.

3.2.2 C_T vs. bead configurations

Figure 11 (a), (b) and **(c)** show the effect of d_{Bo}, $d_{B1/2}$ and h_p on C_T. The d_{Bo} in winecup type bead has a correlation to C_T and an increase in d_{Bo} increases C_T as shown in Fig. 11 (a), although C_T in winecup type is lesser than in well type bead. There is no correlation for both types of bead between $d_{B1/2}$ and C_T as in (b). The h_p in well type bead has a correlation to C_T and an increase in h_p increases C_T as in (c). Now the authors have tried to

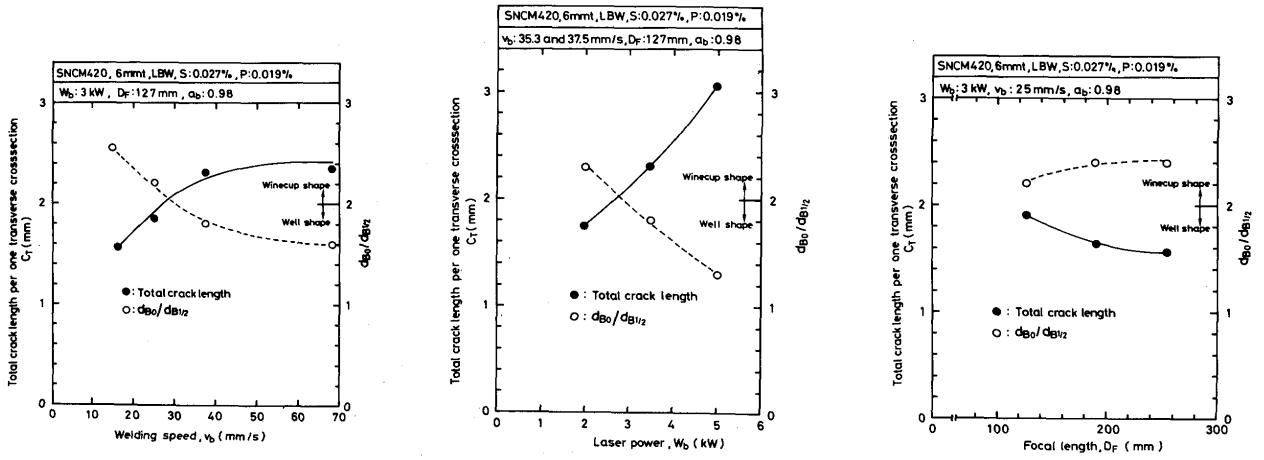

Fig. 9 Welding variables vs. total crack length C_T.

(a) Relation between welding speed and total crack length.
(b) Relation between laser power and total crack length.
(c) Relation between focal length and total crack length.

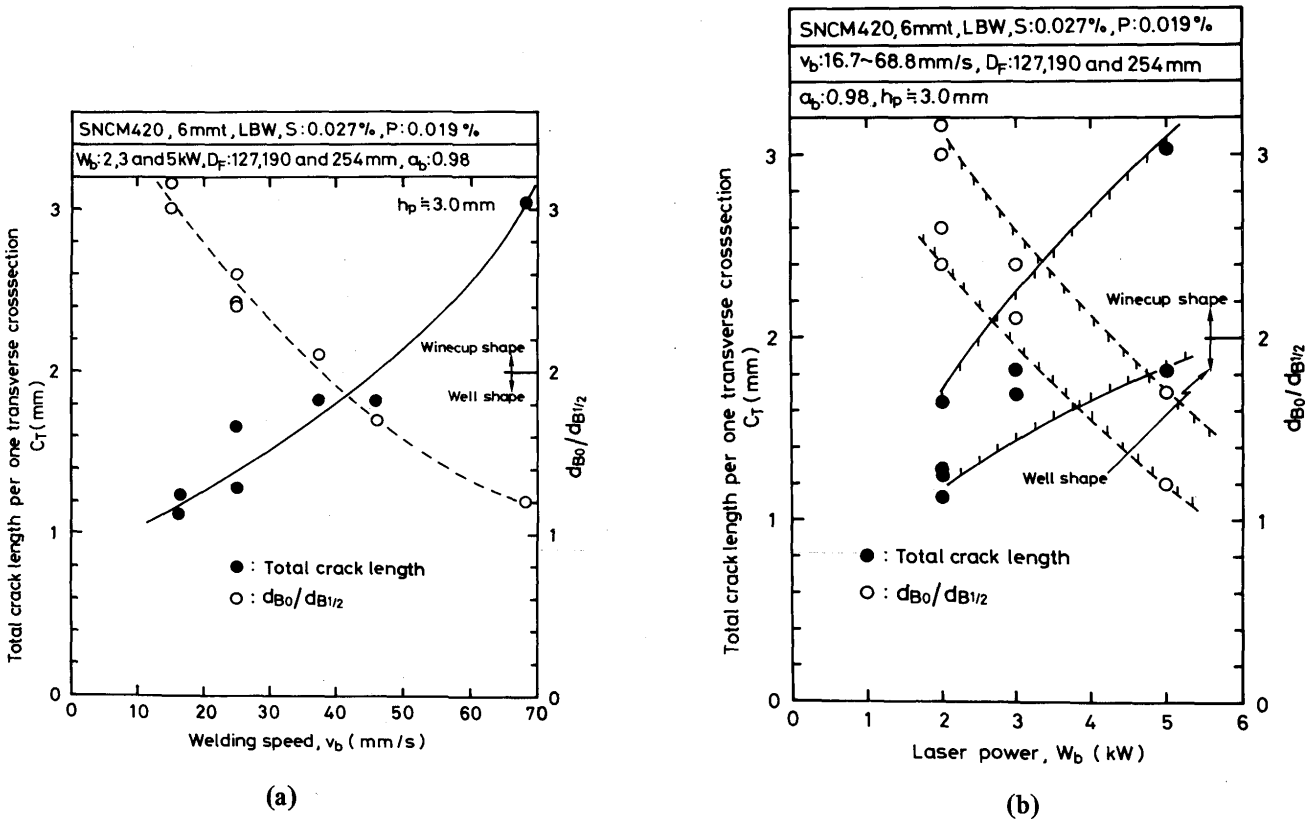

Fig. 10 Welding variables in constant penetration depth vs. total crack length, C_T.

(a) Relation between welding speed and total crack length under the condition of constant penetration depth.

(b) Relation between laser power and total crack length under condition of the constant penetration depth.

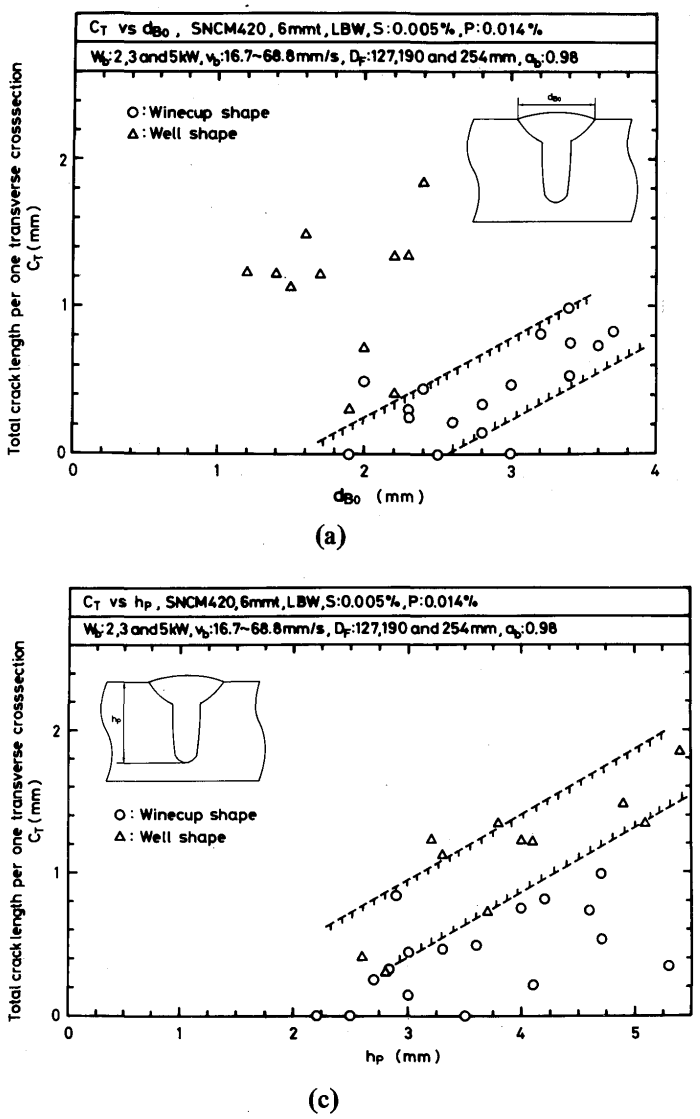

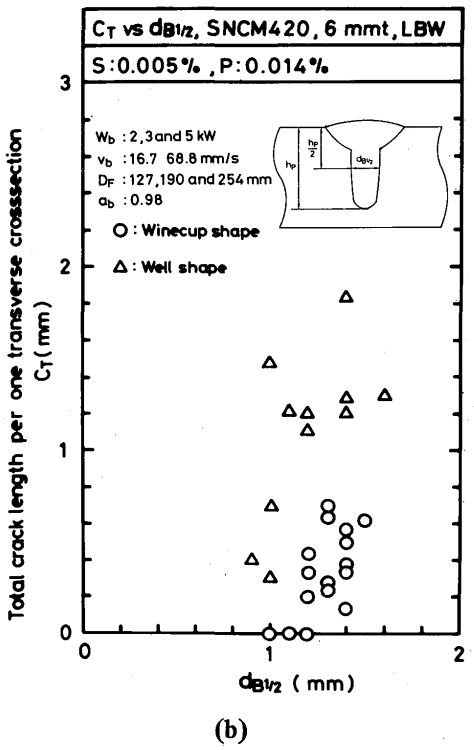

Fig. 11 Bead parameters vs. total crack length, G.
(a) Relation between d_{Bo} and total crack length.
(b) Relation between $d_{B1/2}$ and total crack length.
(c) Relation between h_p and total crack length.

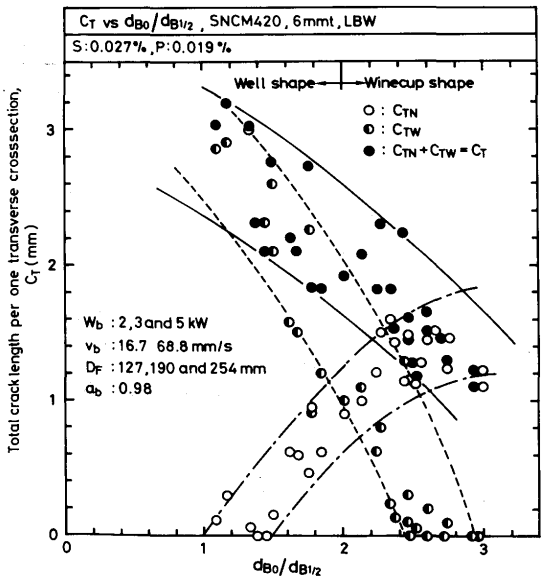

Fig. 12 Relation between $d_{Bo}/d_{B1/2}$ and total crack length.

investigate the relation between the parameter $d_{Bo}/d_{B1/2}$ and C_T. The typical example is shown in **Fig. 12** in which C_T is represented by black marks. C_{TN} and C_{TW} in Fig. 12 are described in 3.3. C_T which is represented by sum of C_{TN} and C_{TW} is decreasing with an increase in $d_{Bo}/d_{B1/2}$ in weld bead, that is to say, C_T of total crack length in weld bead is decreased with a change of bead configuration from "well" to "winecup". There is recognized to have a rough correlation between C_T and $d_{Bo}/d_{B1/2}$.

3.3 Crack length in nailhead (C_{TN}) and well (C_{TW}) parts

3.3.1 Total crack length in nailhead part (C_{TN})

The C_{TN} are represented by d_{Bo} and d_N as in **Fig. 13** (a) and (b). An increase in d_{Bo} and d_N increases C_{TN} sharply at first and reaches to a constant which is depended on S and P contents in steel.

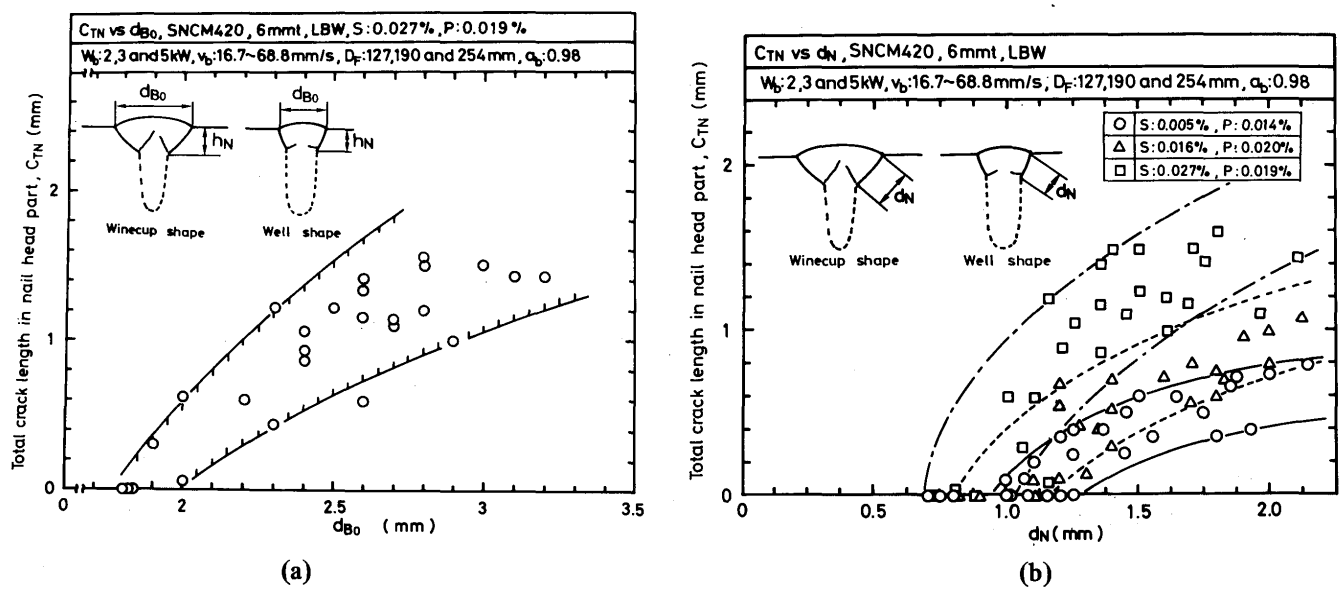

Fig. 13 Bead parameter vs. crack length in nail head part.
(a) Effect of d_{Bo} on total crack length in nail head part.
(b) Effect of d_N on total crack length in nail head part.

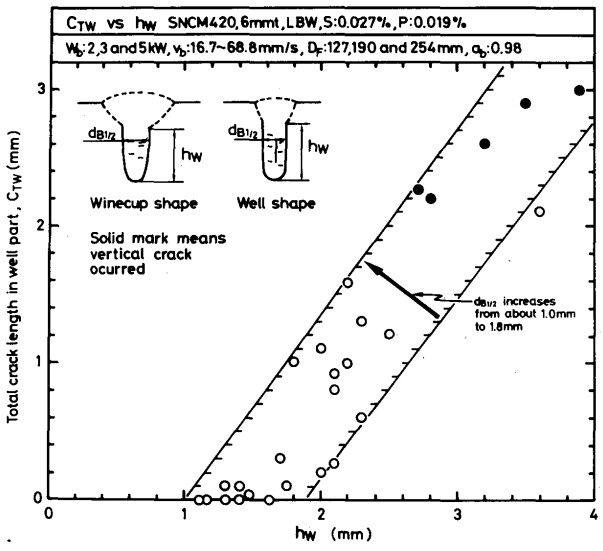

Fig. 14 Effect of h_W on total crack length in well part.

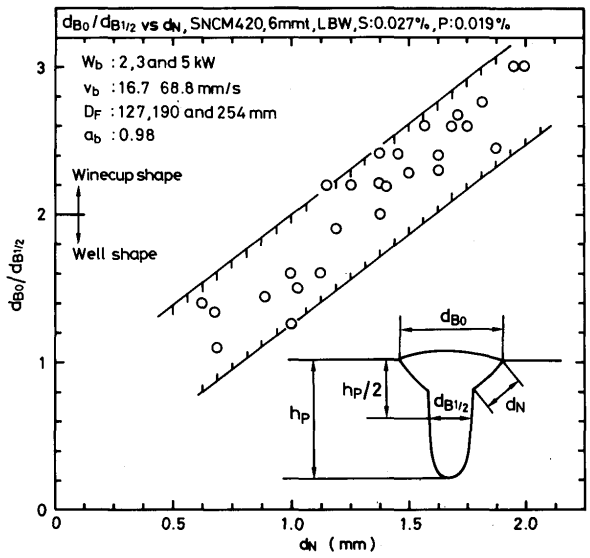

Fig. 15 Relation between d_N and $d_{Bo}/d_{B½}$.

3.3.2 Total crack length in well part

Figure 14 shows the relation between h_W and C_{TW}. An increase in h_W increases C_{TW} and judging from the data an increase in $d_{B½}$ also increases C_{TW} in some scattering range.

The data in black mark indicate the bead in which vertical crack occurs because of wider $d_{B½}$. It seems that C_{TN} is affected by h_W and $d_{B½}$.

3.3.3 C_{TN}, C_{TW} vs. $d_{Bo}/d_{B½}$

The relations between d_N and $d_{Bo}/d_{B½}$ and between $h_W+0.7d_{B½}$ and $d_{Bo}/d_{B½}$ are shown in **Fig. 15** and **16**. There are a close correlation between them. Therefore C_T is also represented by $d_{Bo}/d_{B½}$. As a result, as shown in Fig. 12 C_{TN} and C_{Tw} are shown with $d_{Bo}/d_{B½}$. An increase in $d_{Bo}/d_{B½}$ shows an increase of C_{TN} and a decrease in C_{Tw}. According to Fig. 12, C_T (C_{TN} + C_{Tw}) is strongly depended on C_{Tw} in case of small $d_{Bo}/d_{B½}$ and C_{TN} in case of large $d_{Bo}/d_{B½}$.

3.4 S and P in steel vs. crack susceptibility

3.4.1 $C_T$vs. $d_{Bo}/d_{B½}$

Figure 17 shows the relation between $d_{Bo}/d_{B½}$ and C_T for four different steels of S and P content. An increase in

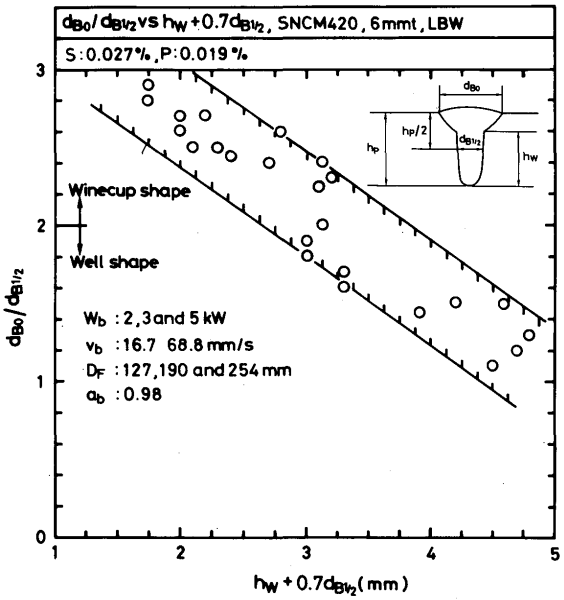

Fig. 16 Relation between $h_W + 0.7d_{B½}$ and $d_{Bo}/d_{B½}$.

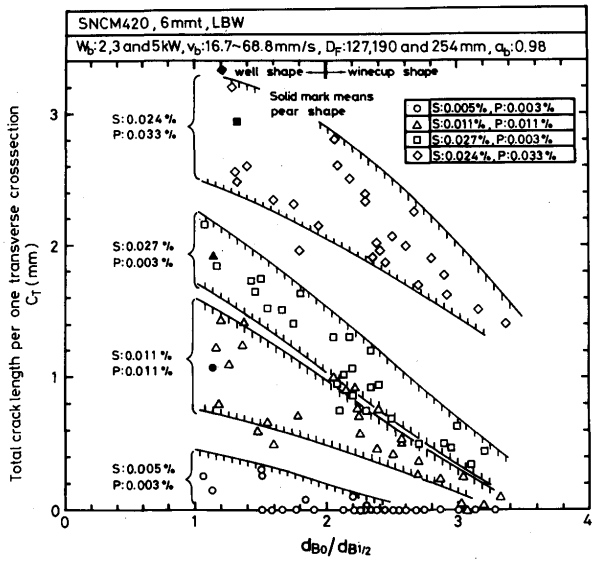

Fig. 17 Effect of S and P content on relation between $d_{Bo}/d_{B½}$ and total crack length.

$d_{Bo}/d_{B½}$ decreases C_T for each steel. Moreover decreasing of S and P greately decreases C_T, that is to say, S and P have a detrimental effect for crack susceptibility in LBW which is well known in arc welding and in EBW.

3.4.2 S vs. P content in C_T

Figure 18 (a) and **(b)** show the effect of S and P on C_T, and (a) for well type bead of about 1.5 of $d_{Bo}/d_{B½}$ and (b) for winecup type of about 2.5 of $d_{Bo}/d_{B½}$. Number in the figure shows C_T and each solid line shows equi-C_T line. According to the figures both S and P have detrimental to solidification crack susceptibility but S shows worse effect than P in general. This means that reducing S is much better than reducing P for solidification crack susceptibility even in these steels.

Square in the figures shows the contents of S and P in commercially available steel at the present.

In Fig. 18 (a) of $d_{Bo}/d_{B½}$ = 1.5 there is no crack-free zone even if reducing S and P in steel, but in Fig. 18, (b) of 2.5 there is crack-free zone in the range of less than 0.005%S and 0.014%P.

Therefore the authors have investigated the crack-free zone in weld bead of various values of $d_{Bo}/d_{B½}$. **Figure 19** shows collectively the crack-free zones for about 2.5,

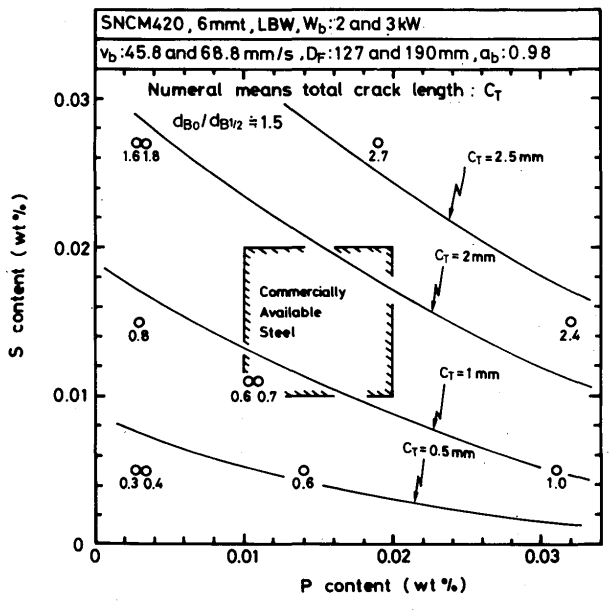

(a)

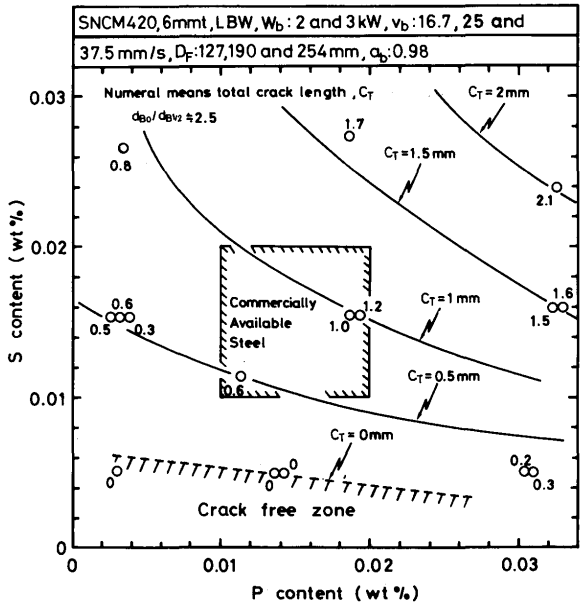

(b)

Fig. 18 Effect of S and P content on total crack length under the conditions of (a) $d_{Bo}/d_{B½}$ = 1.5 and (b) $d_{Bo}/d_{B½}$ = 2.5.

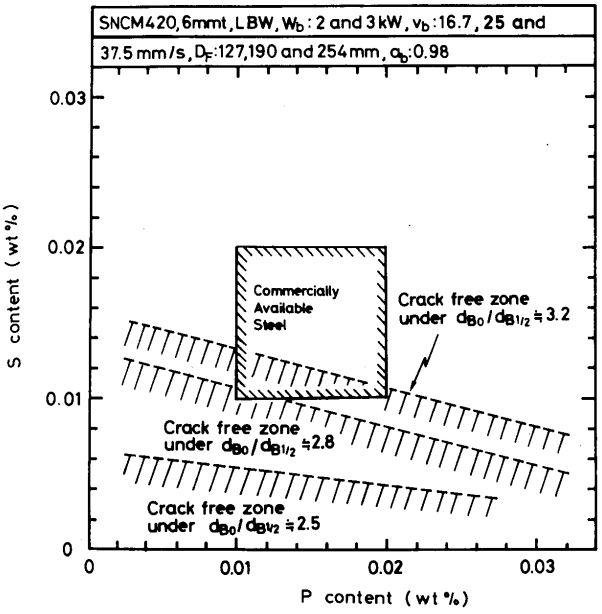

Fig. 19 Effect of $d_{Bo}/d_{B½}$ on crack free zone.

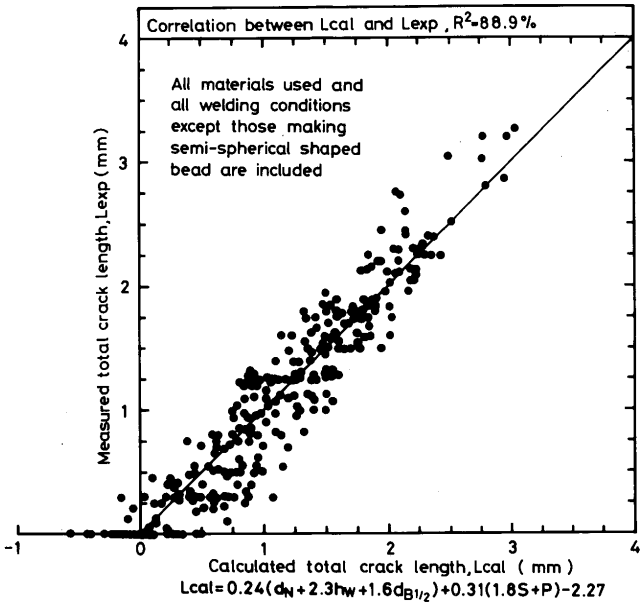

Fig. 20 Correlation between calculated total crack length (L_{cal}) and measured total crack length (L_{exp}).

2.8 and 3.2 of $d_{Bo}/d_{B½}$. Increasing $d_{Bo}/d_{B½}$ the crack-free zone expanded to higher S and P. Especially in the weld bead of 3.2 of $d_{Bo}/d_{B½}$ the crack-free weld can be obtained even in commercial steel at the present. However, as a general description, the commercial steel at the present should be reduced for S, in order to have a much better weld bead by laser beam. Moreover in comparison with Fig. 8, the welding condition which makes bead larger $d_{Bo}/d_{B½}$, that is, lower welding speed, lower power and larger focal length, is better to choice for solidification cracks in weld bead.

3.5 Statistical evaluation for crack susceptibility

Now the authors have tried to investigate statistical evaluation for crack susceptibility using the factors of configuration of bead and S and P contents in 0.2C-low alloy steel.

Figure 20 shows the correlation between measured C_T (L_{exp}) and calculated C_T (L_{cal}) by regression analysis which shows one of the most reliable expressions using both factors for bead configuration of d_N, h_w, $d_{B½}$ and for impurities of S and P in steel. The equation of L_{cal} is given by

$$L_{cal} = 0.24\,(d_N + 2.3h_w + 1.6d_{B½}) + 0.31\,(1.8S + P) - 2.27 \quad (1)$$

In Eq. (1) $d_N + 2.3h_w$ in the first term means the length of side wall of penetration, and then the larger the length, the severer the crack susceptibility.

Moreover the effect of the length of h_w (well part) is about 2.3 times more than d_N (nailhead part). Furthermore bead width in half penetrated depth, $d_{B½}$, also strongly affects the increase in crack susceptibility. Concerning impurities in steel S is about 1.8 times severer than P for crack susceptibility. One of the authors have investigated for crack susceptibility of arc welding before[5] in which S in steel has much detrimental effect comparing with P until about 0.16%C in plain carbon steel. This investigation in Eq. (1) shows much detrimental effect of S is extended to 0.2%C-low alloy steel.

Next, some researchers represented the crack susceptibility in electron beam weld bead by $d_{Bo}/d_{B½}$[6,7] and in this investigation the authors agreed with the representation that the factor $d_{Bo}/d_{B½}$ will show one of bead configuration in LBW. Therefore another regression analysis was tried using $d_{Bo}/d_{B½}$. The result is shown in **Fig. 21**. This has also a good correlation. Increasing $d_{Bo}/d_{B½}$ decreases L_{cal}.

L_{cal} is given by

$$L_{cal} = -0.67d_{Bo}/d_{B½} + 0.32\,(1.8S+P) + 1.13 \quad (2)$$

Although scattering of the date in Eq. (2) is a little larger than that in Eq. (1) as shown in R, the rough estimation of solidification crack susceptibility of weld bead in LBW will be possible with Eq. (2).

3.6 Effect of restraint during LBW

The experimental results in 3.2 to 3.5 were obtained under a restraint of specimen. Therefore the authors have tried to compare the crack susceptibilities between the

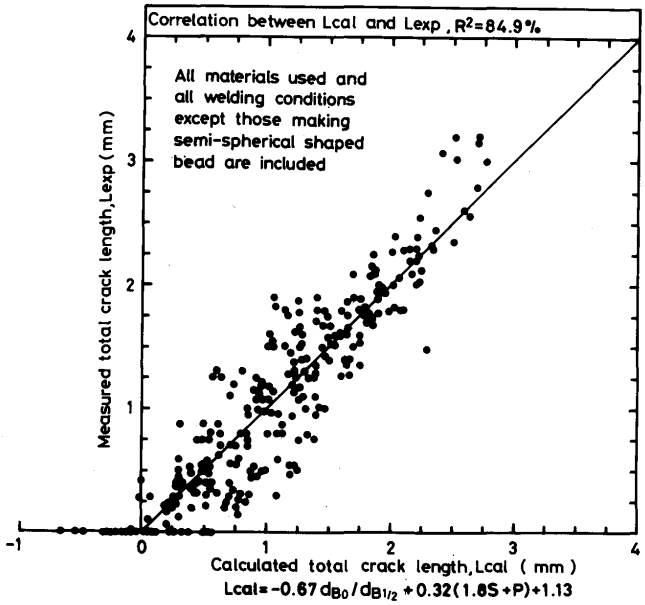

Fig. 21 Correlation between calculated total crack length by use of $d_{Bo}/d_{B½}$ (L_{cal}) and measured total crack length (L_{exp}).

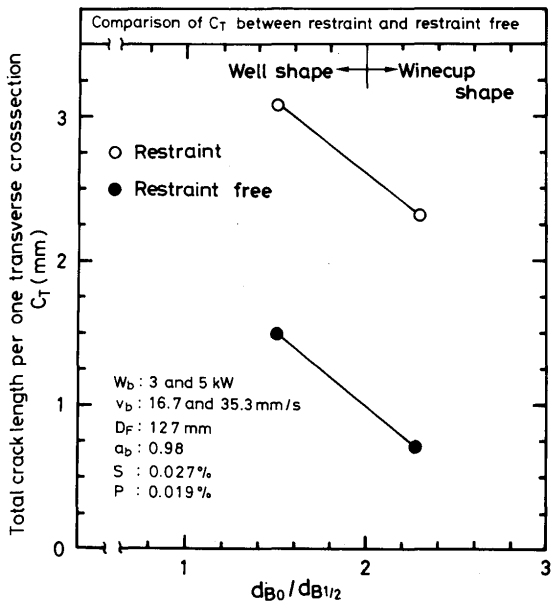

Fig. 22 Comparison of total crack length between restraint and restraint free condition.

restraint and the restraint free weld beads during LBW using same sized specimen.

Figure 22 shows the comparison of C_T against $d_{Bo}/d_{B½}$ for restraint and restraint free beads.

From the figure it is clear that the restraint free bead is much lesser in solidification crack susceptibility than the restraint bead in both well and winecup shaped bead configuration.

According to more precise investigation of crack lengths of both nailhead and well parts, those in the restraint free bead are also lesser than in the restraint bead in the same fashion in both parts. As a result, the fixture of the specimen with a jig increases solidification crack susceptibility in LBW.

In actual LBW, however, the joint to be welded has usually a large restraint, and then the restraint weld bead in this investigation will be realistic.

4. Conclusions

Solidification crack susceptibility of bead-on-plate weld bead by LBW has been investigated under the restraint condition for 6mm thick 0.2%C-Ni-Cr-Mo low alloy (JIS SNCM 420) with various S and P contents. The effects of welding variables, bead configurations and S and P contents on the crack susceptibility were treated. Main conclusions obtained are as follows;

(1) Weld bead configuration is gradually changed from winecup-to well-type with changing to higher power and higher welding speed in LBW within the welding condition in this investigation.

(2) With an increase in weld power and welding speed solidification crack susceptibility in weld bead is increased. This tendency is the same even in the same penetration depth of weld bead. Moreover the welding variables effect the configuration of weld bead, especially in $d_{Bo}/d_{B½}$ of bead width.

(3) Solidification cracks have been seen in both winecup- and well-type weld bead. However, the cracks were much more in well-type bead than in winecup-type bead in general.

(4) S and P impurities in steel have a detrimental effect for the cracks. However S is 1.8 times more detrimental than P according to statistical investigation. Decreasing S in steel is required in order to make the sound weld bead.

(5) According to statistical investigation the cracks increase with an increase in length of side wall fused and of $d_{B½}$ (bead width in ½ penetration)

(6) The equation which can estimate the crack length in weld bead is introduced from the statistical investigation using the factors of bead configuration and impurities (S, P) in steel.

(7) The restraint of the specimen during welding increases the crack susceptibility in weld bead in comparison with the restraint free bead. The effect of the restraint of weld bead in LBW on the crack susceptibility is future investigation.

Acknowledgement

The authors wish to thank Mr. I. Ikegami, and Y. Kotetsu of Niigata Eng. Co. Ltd. for their cooperation for LBW, and Nippon Steel Cooperation for his support of the steels investigated.

References

1) N. Niimi et al: J. Welding Eng. (in Japanese), 4 (1986) P. 60
2) J. Mazumder et al: W. J., 70 (1981) 6, P. 19
3) V. G. Fedorov et al: Avt. Svarka (1984) 10, P. 5
4) F. Matsuda et al: Trans. JWRI, 7 (1978) 1, P. 59
5) F. Matsuda: "Welding Metallugy" (1972), P. 158 Nikkan Kogyo Shinbun (in Japanese)
6) T. Shida et al: J. JWS (in Japanese), 49 (1980) 7, P. 440
7) V. I. Markhnenko et al: Avt. Svarka (1985) 6, P. 43